PCCP

Accepted Manuscript

ROYAL SOCIETY OF CHEMISTRY

www.rsc.org/pccp

Characterization of gas phase WC^{2+}: a thermodynamically stable carbide dication

S. Sabor [1,2], A. Touimi Benjelloun [2], M. Mogren Al Mogren [3] and M. Hochlaf [1,*]

[1] Université Paris-Est, Laboratoire Modélisation et Simulation Multi Echelle, MSME UMR 8208 CNRS, 5 bd Descartes, 77454 Marne-la-Vallée, France

[2] Equipe de Chimie Informatique et Modélisation (ECIM). Laboratoire d'Ingénierie des Matériaux, de Modélisation et d'Environnement (LIMME), Faculté des Sciences Dhar El Mahraz (FSDM), Université Sidi Mohammed Ben Abdallah (USMBA), B.P. 1796, Fès-Atlas, Fès - Maroc.

[3] Chemistry Department, Faculty of Science, King Saud University, PO Box 2455, Riyadh 11451, Kingdom of Saudi Arabia

* author for correspondence:

M. Hochlaf: phone: +33 1 60 95 73 19. FAX: +33 1 60 95 73 20. Email: hochlaf@univ-mlv.fr

Abstract

Using an ab initio methodology, we performed a detailed theoretical study of gas phase WC^{2+} dication. These calculations were done using a multiconfigurational method in connection with a large basis set, where relativistic effects were taken into account. This dication is identified here as the first thermochemically stable doubly charged diatomic carbide in gas phase. Our work confirms hence the stability of this dication in gas phase and its earlier observation by atom probes mass spectrometry. Our calculations show that the shape of the potential energy curves of its lowest electronic states change drastically upon consideration of relativistic effects. For instance, the electronic ground state possesses a Morse-like potential without spin-orbit that evolves to the usual *volcanic* behavior with a columbic 1/R evolution at large internuclear separation after inclusion of spin-orbit. We predict a set of thermochemical and spectroscopic data for this molecular species.

I. Introduction

Small molecular dications, AB^{2+}, are a priori not stable because of the columbic repulsion between the two positive charges. Observation and identification of long-lived AB^{2+} ions intrigued and still intrigue scientists. During the last decades, the spectroscopy and the reactivity of doubly charged molecular ions gained importance. They evolved from simple curiosity to chemical species relevant for several media and a variety of fields. They present specific physical and chemical properties that are important for a wide range of potential applications. All these features were recently illustrated and highlighted in the PCCP themed issue on multi charged ions organized by Price and Roithová [1]. We refer to the Editorial of this themed issue for further illustration of the recent achievements on the investigation of the spectroscopy and the reactivity of doubly charged molecules [2]. As shown there, theoretical chemistry, in connection with state-of-art experimental studies, played a crucial role for elucidation and explanation of their metastability and reactivity.

In 1998, Schröder, Harvey and Schwarz [3] showed that there are three classes of diatomic dications: "stable", "metastable" and "unstable". This classification is based on the existence or not of a potential well along the internuclear separation and on the relative energy position of this minimum with respect to the lowest dissociation limit. Mostly, AB^{2+} stability can be discussed in terms of the order of ionization energies of the separated atoms. For instance, thermodynamically stable AB^{2+} are formed when the second ionization of A (assumed having the lowest first ionization energy) is smaller than the first ionization energy of B. This ground state electronic potential correlates to the charge retaining channel (A^{2+} + B) at large internuclear separations. The charge separation channel (A^{+} + B^{+}) is located therefore higher in energy and there are no crossing between this potential and the 1/R columbic explosion evolution. Therefore, a Morse-like potential is expected because of the attractive character of the bonding between the A^{2+} and B species. The dication is named "thermodynamically stable", which is also the case when the crossing between both diabatic curves is located at large R's. Readers are referred to the recent review by Sabzyan, Keshavarz and Noorisafa [4] for further details and examples. Generally, previous works established that stability can be acquired either by increasing Z of A and / or B atoms or by increasing the size of the molecule. In both cases, double ionization energies are more rapidly lowered compared to single ionization energies.

Strictly speaking, only dications having Morse-like potentials can be considered as stable since the others present some rovibrational levels that have finite lifetimes because of tunneling through the potential barrier. To date, few thermochemically stable diatomic dications are identified. They consist mainly on fluorine diatomics, XF where X = M (metal e.g. Al, Be) or Ca or Si since X presents a low ionization energy to form X^{2+} from X^{+} compared to the relatively high ionization energy of fluorine (17.4 eV [5]). Presently, we predict a thermochemically stable non-fluorine dication, namely the tungsten carbide dication, WC^{2+}. The neutral tungsten carbide (WC) is relevant for industrial and catalytic domains due to its unusual properties, such as high melting point, superior

hardness, low friction coefficient, high oxidation resistance and good electrical conductivity [6]. The full understand of this material is crucial for these wide ranges of applications. It is worth hence to investigate the thermochemical and spectroscopic properties of WC and related ionic species with modern theoretical methodologies.

Back to the seventies, WC^{2+} was observed with atom probe mass spectrometry [7,8]. In the begging of the 90th, WC^{2+} was formed by charge transfer reactions between doubly charged rare gas projectile ions and $W(CO)_6$ [9,10]. These works provided the ionization/appearance energies of W^+, W^{2+}, WC^+, WC^{2+} and of several $(CO)_xW^{q+}$ (q=1,2) singly and doubly charged intermediate ions. Nevertheless, the error bars of these determinations remained quite large (of ±0.8 eV). Very recently, WC^{2+} was detected by mass spectrometry through atom probe tomography analysis of WC powder [11] and electron impact ionization of $W(CO)_6$ molecular beam [12]. The latter work reinvestigated the electron impact induced reactions identified by Cooks and co-workers [9,10]. These authors gave more precise values for the appearance energies of the ionic species (including W^+, W^{2+}, WC^+, WC^{2+}) where the experimental error bars on the appearance energies were reduced to ± 0.12 eV. In 1997, Qi et al. [13] performed a synchrotron vacuum ultraviolet photoionization and dissociative photoionization of gas phase $W(CO)_6$. They did observe some of $(WC_m(CO)_n)^{q+}$ (q=1,2) precursors formed in the earlier and recent electron impact experiments but not WC^{2+}. No explanation is given there for that.

There were no theoretical investigations of the WC^{2+} dication since its discovery. In this theoretical contribution, we treat the lowest electronic states of WC^{2+} using multi-reference configuration interaction theoretical techniques combined with large basis sets, where spin-orbit interactions were considered. Several potential wells are found and we definitely establish WC^{2+} as a stable dication in gas phase. The effect of the spin-orbit effects on the shape of the potentials is deeply investigated. Finally, we provide the double ionization energies for WC and a set of spectroscopic parameters for WC^{2+}, which includes equilibrium distances, vibrational and rotational terms, excitation and dissociation energies.

II. Theoretical approaches

All electronic computations were performed using the MOLPRO package (version 2012.1) [14]. The electronic computations were carried out in the C_{2v} point group, where the B_1 and B_2 representations are equivalently treated.

The carbon atom is described by the aug-cc-pV5Z basis set [15,16]. For tungsten atom, we used the recently released basis set aug-cc-pV5Z-PP by Figgen et al. in connection with the fully relativistic ECP60MDF pseudo potential [17]. Here, the 60 core electrons are represented by a pseudopotential and the 14 outer electrons are explicitly treated via the associated contracted basis sets corresponding to the scheme (17s14p12d5f5g3h2i)/[8s8p7d5f4g3h2i]. This results in 324 Contracted Gaussian Type Orbitals (cGTOs) to be considered. In total, eighteen electrons were correlated. Previously, benchmark computations on several metal containing metals dealing with their

energetics (electron affinities, ionization energies) and their spectroscopic parameters showed that the results from the pseudopotential and all-electron calculations were nearly identical when scalar relativity was accurately included in the all-electron work [18-20].

In order to account for the multiconfigurational nature of the wavefunctions of the electronic states of WC^{2+}, we used the complete active space self-consistent field (CASSCF) [21,22], followed by the internally contracted multi-reference configuration interaction technique [23,24]. For better accuracy, we quoted the values after consideration of the Davidson correction (MRCI+Q) [25]. In CASSCF, the active space was constructed by considering the 5d and 6s atomic orbitals (AOs) of W and 2s and 2p AOs of C as active. The inner shells were kept frozen. Thus, the active space consisted of (4-8)σ, (2-4)π and 1δ molecular orbitals (MOs). All electronic states having similar spin-multiplicity were averaged together with equal weights using the state-averaging procedure of MOLPRO. Thus, we treated more than 5000, 2000 and 300 Configuration State Functions (CSFs) per C_{2v} symmetry when computing the triplet, quintet and heptet states of WC^{2+}, respectively. In MRCI, all CSFs from the CASSCF wavefunctions were considered as a reference. Hence, we took into account hence more than 2.5 x 10^8 (4.2 x 10^6), 1.4 x 10^8 (4.4 x 10^6) and 3.1 x 10^7 (1.3 x 10^6) uncontracted (contracted) CSFs per C_{2v} symmetry when computing the triplet, quintet and heptet electronic states of WC^{2+}. In our benchmark computations on XO^{q+}(q=2,3,4 and X = Nb, Re and Hf), we showed that this methodology is accurate enough to correctly account for electron correlation and relativistic effects of multi charged molecular systems that contain heavy metal atoms [26]. In related topic, tests computations on IO($X^2\Pi$) and on $CF_3I(X^1A_1)$ benchmarked by experimental data confirmed also these assumptions [27,28].

For the estimation of the spin-orbit coupling on the low electronic states of WC^{2+}, we evaluated the spin-orbit coupling matrix elements in Cartesian coordinates, where the CASSCF wavefunctions were used as the multi-electron basis for the two-step spin-orbit coupling calculations [29,30] at the level of Breit-Pauli Hamiltonian [31]. The Ω spin-orbit eigenstates were derived after diagonalization of the electronic Hamiltonian including the spin-orbit operator in the basis of the CASSCF unperturbed wavefunctions.

Finally, the potential energy curves (PECs) were incorporated to solve the one-dimensional Schrödinger equation for the nuclear motion problem [32,33]. Hence, we deduced hence a set of spectroscopic constants for the Λ-Σ and Ω bound states of WC^{2+} dication. These constants were obtained using the derivatives at the minimum-energy distances and standard perturbation theory.

III. Results and discussion

1. Benchmark calculations on the energetics of W, W^+ and W^{2+}

As test of the energetics issued from the present procedure, we computed the energy separations between the J states of W(^{5}D, ^{7}S, ^{3}P, ^{3}F), W^+(^{6}D, ^{6}S) and W^{2+}(^{5}D, ^{3}P) induced by spin-orbit effect. These calculations were carried out at the CASSCF/aug-cc-pV5Z(-PP) and MRCI/aug-cc-

pV5Z(-PP) levels. The results are listed in Table 1 where they are compared to the experimental data [34-36]. This table shows that the inclusion of spin-orbit couplings is mandatory to account for the splitting and for the correct ordering of the J states. For instance, the ground state of neutral W is ^7S without spin-orbit correction whereas it turns out to be the $^5D_0$ component, followed by the $^5D_1$ and then the $^7S_3$ components as established experimentally. Moreover, this table reveals that the errors between the computed and the measured values are less than 10 % for neutral W whereas deviations reach 30% for some J-states of W^+ and W^{2+}. Such discrepancies are not surprising for this heavy 5d element since the set of atomic data used for the optimization of the aug-cc-pV5Z(-PP) basis set [17] does not include the W^{2+} dication and the specific spin-orbit structure of the W^+ and W^{2+} ions. As pointed out by Figgen et al, this may be due to relatively strong configurational mixing among SO states of W^+ and W^{2+} which is accounted for only via a proper treatment of SO effects. Anyway, the actual description of this effect should be largely enough to deduce accurate energetics for WC^{2+}.

Table 2 lists the first (IE1) and the second (IE2) ionization energies of W(^7S, ^5D) with and without spin-orbit. IE1 corresponds to the energy difference between neutral W and W^+ and IE2 is for the energy difference between W and W^{2+}. For the $W(^5D_0) \rightarrow W^+(^6D_{1/2}) + e^-$ ionization reaction, we compute IE1 of 7.93 eV at the MRCI/aug-cc-pV5Z(-PP) and after considering spin-orbit effects. This IE agrees well with the commonly admitted measured value for the first ionization energy for W (of 7.86403 eV). This good agreement is expected since the aug-cc-pV5Z-PP and corresponding pseudopotential for W were optimized to reproduce this quantity. At the MRCI+SO/aug-cc-pV5Z(-PP) level, we compute IE2 of 23.04 eV for the $W(^5D_0) \rightarrow W^{2+}(^5D_0) + 2e^-$ double ionization process and an IE2 of 24.15 eV when the upper $^5D_4$ component of W^{2+} is produced. Our IE2 are within the average values of the experimental IE2 determinations. Indeed, different IE2(W) values were deduced with relatively large error bars because of the difficulty to get such quantity from experiment. For instance, Kramida and Shiri [37] measured IE2(W) = 24.33 ± 0.15 eV and Lide referenced IE2(W) = 23.96 ± 0.4 eV [38] where atomic W is produced in gas phase in a hollow cathode. The exact mechanism and therefore the exact quantum state of neutral W prior to ionization are not well identified in such plasma. We may expect a large population distribution over the low J-states of W. This makes somehow the comparison to the theoretical values quite hard.

2. On the electronic states of WC^{2+}

Figures 1 and 2 display the MRCI+Q/aug-cc-pV5Z(-PP) (Λ - Σ) PECs and the Ω PECs of the lowest electronic states of WC^{2+} vs. the internuclear distance. In both figures, the reference energy is chosen to be the energy of respective WC^{2+} ground state at equilibrium. The dissociation limits $\{W^+(^6S_u)+C^+(^2P_u), W^+(^6D_u)+C^+(^2P_u), W^{2+}(^5D_g)+C(^3P_g)\}$ were positioned using the MRCI data on W^+ and W^{2+} given in Table 1 and those on C and C^+ (not shown here). Accordingly, the charge separation channels $\{W^+(^6S_u)+C^+(^2P_u)$ and $W^+(^6D_u)+C^+(^2P_u)\}$ are located at ~0.86 eV and the charge retaining asymptote $\{W^{2+}(^5D_g)+C(^3P_g)\}$ is located at ~5.11 eV. After considering the spin-orbit interaction, the lowest components of $W^+(^6D_u)+C^+(^2P_u)$ {i.e. for $W^+(^6D_{1/2}) + C^+(^2P_u)$} and of $W^{2+}(^5D_g)+C(^3P_g)$ {i.e.

$W^{2+}(^5D_0)+C(^3P_g)\}$ and the $W^+(^6S_{5/2})+C^+(^2P_u)$ limit are located at ~0.53 eV, ~4.79 eV and 1.78 eV, respectively. The other asymptotes are positioned using the excitation energies listed in Table 1. The spin-orbit effects on C and C^+ are small and cannot be clearly evidenced in Figure 2.

Similar to neutral WC [39], the ground state of WC^{2+} is the $X^3\Delta$ state (Figure 1). Table 3 lists the dominant electron configurations of the doubly charged WC^{2+} $\Lambda - \Sigma$ states quoted at the equilibrium distance of WC^{2+} ground state. The wavefunction of $WC(X^3\Delta)$ neutral species is dominantly described by the $4\sigma^2\ 2\pi^4\ 5\sigma^2\ 1\delta^1\ 6\sigma^1$ electron configuration. The formation of the $WC^{2+}(X^3\Delta)$ electronic state corresponds to the removal of one electron from the 6σ MO and a second electron from the 5σ MO, resulting on the $4\sigma^2\ 2\pi^4\ 5\sigma^1\ 1\delta^1\ 6\sigma^0$ electron configuration. Figure 3 depicts the outermost MOs of WC. This figure reveals that the 1δ MO is non-bonding and that the 5σ MO is slightly bonding in nature whereas the 6σ MO is slightly anti-bonding. Therefore the equilibrium distances of WC and WC^{2+} are expected to be close (see below). For the $1^3\Pi$, $1^3\Phi$, $1^5\Pi$ and $1^5\Sigma^+$ states, they are formed after ejection of one electron from 6σ and a second one from the other outermost MOs of WC with simultaneous internal electron excitation within these MOs. For the $1^3\Sigma^+$, $1^7\Sigma^+$, $1^5\Delta$ and $1^7\Pi$ states, both electrons are removed from the inner-valence MOs of neutral WC. Table 3 gives also the vertical excitation energy of WC^{2+} states with respect to $WC^{2+}(X^3\Delta)$ minimum energy.

The $WC^{2+}(X^3\Delta)$ electronic state correlates adiabatically to the charge retaining dissociation limit, $W^{2+}(^5D_g)$ + $C(^3P_g)$. It presents a Morse-like potential with a deep potential well. The depth of this potential well is ~5.1 eV. After considering spin-orbit, there is a drastic change in the shape of the ground state of this dication from Morse-like to *volcanic* shape with the usual 1/R evolution (Figure 4), especially at large internuclear separations. Indeed, the ground state corresponds to Ω = 1 component arising from the levy of degeneracy of WC^{2+} $(X^3\Delta)$. The potential energy curve of this component follows more or less the $X^3\Delta$ PEC for internuclear distances smaller than ~5.5. For R_e > 5.5 bohr, the Ω = 1 component comes from the quintet states that correlate to the lowest dissociation limit. Additional avoided crossings between the Ω = 1 components coming from the electronic excited Λ - Σ states are also evidenced in Figure 2.

Interestingly, the bound ground minimum, and especially the v=0 level (Figure 4), lies lower in energy than the lowest atomic asymptote whenever we consider $\Lambda - \Sigma$ or Ω PECs. Thus, our calculations reveal the existence of a thermochemically stable diatomic dication in gas phase. The WC^{2+} carbide is the first stable non-fluorine dication. In the literature, the stability of metal fluorides dications (MF^{2+}) is explained by the relatively low ionization energies (IEs) of M^+ to the corresponding dications M^{2+}, while the IE(F) is high (=17.4 eV [5]). The present case shows that stable dications can also exist when the ionization energy of the non-metallic atom is not that high (e.g. IE(C) =11.26 eV [5]).

The fragmentation energy of WC^{2+} ground state corresponds to two distinct quantities: without spin-orbit effect, it can be associated with the dissociation energy (D_e) of a Morse-like potential. D_e is calculated hence as the energy difference between the energy at equilibrium and the energy at the corresponding dissociation limit {i.e. $W^{2+}(^5D_g)$ + $C(^3P_u)$}. When spin-orbit effect is taken into account, the fragmentation energy matches as the kinetic energy release (KER). KER is deduced as the difference energy between the energy at the max of the potential and the $W^+(^6D_{1/2})$ + $C^+(^2P_u)$ dissociation energy. Here, we compute D_e ~5.10 eV and KER ~3.65 eV. Note that D_e is a hypothetical thermodynamical parameter since solely KER can be accessed by experiment. Anyway, this potential well is deep enough to support several rovibrational levels where long-lived WC^{2+} may be formed. The PECs of the triplet excited states present similar behavior after considering the spin-orbit interaction. The dissociation energies of the triplet states that turns out to be KERs as for the ground state are reduced after consideration of relativistic effects.

More generally, Figure 1 shows a high density of $\Lambda - \Sigma$ electronic states in the 0 – 4 eV energy range. It results in a dense manifold of Ω states and therefore in several avoided crossings between the PECs having the same Ω (Figure2). Such interaction leads to the odd shape of some Ω components (e.g. Ω = 0 PECs except the lowest one). Moreover, these avoided crossings upon consideration of spin-orbit effects lead to the formation of additional potential wells. For instance, the avoided crossings between the Ω = 3 PECs result in potential minima with increasing equilibrium internuclear separations ranging from 3.3 bohr for the lowest component to 4.75 bohr to the upper one (Figure 2). At these avoided crossings, vibronic couplings are expected to take place.

3. Spectroscopic parameters

Table 4 lists the spectroscopic constants of the electronic states of WC^{2+} dication derived from our MRCI+Q potentials. This includes the equilibrium distances (R_e), the rotational constants (B_e), the vibration-rotation terms (α_i), the harmonic frequencies (ω_e), the anharmonic terms ($\omega_e x_e$). For ground state, it splits into three components, namely Ω=1, 2 and 3. At equilibrium, we evaluate a splitting of ~ 0.27 eV between the Ω=1 and Ω=2 components and of 0.52 eV between Ω=2 and Ω=3 (Table 4). These splittings are consistent with those of neutral $WC(X^3\Delta)$, for which Balasubramanian [39] calculated splittings of 0.20 eV and 0.34 eV, respectively. For the dicationic upper states, the spin-orbit splittings can be deduced from Figure 2 and Table 4.

Generally, the consideration of spin-orbit effect does affect only slightly the spectroscopic properties of the unperturbed $\Lambda - \Sigma$ states, which are deduced from the derivatives at equilibrium. Indeed, the spin-orbit effect more or less disturbs the shape of the WC^{2+} unperturbed states close to equilibrium and it is effective at large internuclear distances where it results in the drastic changes in the shapes of the perturbed PECs as noticed above. For instance, we compute an equilibrium distance for $WC^{2+}(X^3\Delta)$ of 1.736 Å. The consideration of the spin-orbit effect leads to a slightly longer WC equilibrium distance (R_e) for the lowest Ω=1 component (of 1.744 Å). Similarly, the computed

harmonic frequency for $WC^{2+}(X^3\Delta)$ (ω_e = 1008 cm^{-1}) is also close to the one computed for WC^{2+} (X Ω = 1) (of 1003 cm^{-1}).

Because of their close interactions and for most of Ω components, the shape of their potentials is far from common anharmonic potential well. For some of them, this results on large $\omega_e x_e$ terms and even in inverted anharmonicities. Similarly, the rotation-vibration terms (α_e) are also either positive or negative. Note that the $\omega_e x_e$ and α_e terms should be viewed as indicative. For the location of the rovibrational levels on the corresponding potentials, one may incorporate our potentials into a variational treatment of the nuclear motions. For that purposes, our PECs can be sent upon request.

4. Double ionization energies of WC

In the literature, solely the appearance energy (AE) of WC^{2+} is known. This quantity is determined however with quite large error bars (ranging from ± 0.8 eV till ± 0.12 eV) through impact ionization of gas phase $W(CO)_6$ or charge transfer reactions between doubly charged rare gas projectile ions and $W(CO)_6$ [7-10,12]. AE corresponds to the energy for the formation of WC^{2+} after complex reactive processes and hence there is no direct measurement of the double ionization energy of WC in the literature.

At present, we determine both the vertical double ionization energy (VIE2) and the adiabatic double ionization energy (AIE2) of WC. VIE2 is evaluated as the energy difference between the energy of WC^{2+} ground state and the energy of WC ground state at the equilibrium geometry of the neutral molecule. AIE2 corresponds to the difference between the energy of WC^{2+} ground state and the energy of WC ground state taken at their respective equilibrium and after considering the zero-point vibrational energy correction (ZPE). At the MRCI+Q/aug-cc-pV5Z(-PP) level, VIE2 and AIE2 are computed to be 23.57 eV and 23.56 eV, respectively. These energies are close to each other because the equilibrium distances of neutral WC ($X^3\Delta$) (R_e= 1.727 Å [39]) and of WC^{2+} ($X^3\Delta$, R_e= 1.736 Å) dication are close. After considering the spin-orbit effect, VIE2 and AIE2 remain sensitively unchanged since this interaction affects the ground states of WC and WC^{2+} with similar splitting (see above). They are slightly reduced to VIE2=23.50 eV and AIE2=23.49 eV. These values are recommended to be compared to experimental values whenever measured.

IV. Conclusions

The present large ab initio computations confirm the existence of WC^{2+} dication in gas phase. More interestingly, we show that WC^{2+} is thermodynamically stable, being hence the first stable doubly charged carbide. We predict several deep potential wells where electronically excited WC^{2+} can be found. In addition, our theoretical results reveal that the consideration of spin-orbit effects changes the shape of some potential energy curves from Morse-like to *volcanic*. For instance, this is the case of the dicationic ground state potential. Therefore, one cannot omit to take into account such interaction for the good description of organometallic dications. Specifically, this work shows that the WC^{2+} dication presents a specific behavior leading to a stable character. This is worth to study for the

other 5d transition metal carbide multi-charged ions and to draw general trends if any.

Moreover, we derived an accurate set of spectroscopic parameters. We also determined precisely the double ionization energies of W and of WC. Determination of precise energetics for these species is important for the estimation of the bond dissociation energies of organometallic complex (e.g. $W(CO)_6$) under VUV radiation or electron impact. These quantities are relevant for instance for reactivity and catalysis.

Acknowledgements

The authors would like to extend their sincere appreciation to the Deanship of Scientific Research at King Saud University for its funding the research through the Research Group project No. Research group no RGP-VPP-333. This research was supported by a Marie Curie International Research Staff Exchange Scheme Fellowship within the 7th European Community Framework Program under Grant No. PIRSES-GA-2012-31754, the COST Action CM1002 CODECS. We thank Roberto Linguerri (Université Paris-Est) for valuable discussions.

References

1. Phys. Chem. Chem. Phys. **13** (2011).
2. S. D. Price and J. Roithová. Phys. Chem. Chem. Phys. **13**, 18251–18252 (2011).
3. D. Schröder, J. N. Harvey and H. Schwarz. J. Phys. Chem. A **102**, 3639-3642 (1998).
4. H. Sabzyan, E. Keshavarz and Z. Noorisafa. J. Iran Chem. Soc. **11**, 871 (2014).
5. http://webbook.nist.gov.
6. W. J. Balfour, J. Cao, C. V. V. Prasad, and C. X. Qian, J. Chem. Phys. **103**, 4046 (1995).
7. E. W. Müller, S. V. Krishnaswamy and S. B. McLane, 32nd Physical Electronics Conference, NBS, Washington, D.C., Mar. 1971.
8. E. Müller and T. T. Tsong, Progress in Surface Science **4**, 1 (1974).
9. S. R. Horning, T. Kotiaho, L. E. Dejarme, J. M. Wood and R. G. Cooks. Int. J. Mass Spectro. and Ion Processes **110**, l-29 (1991).
10. R.G. Cooks, T. Ast, B. Kralj, V. Kramer and D. Zigon, J. Am. Sot. Mass Spectrom. **16**, 1 (1990).
11. J. Weidow. Ultramicroscopy **132**, 295–299 (2013).
12. K. Wnorowski, M. Stano, W. Barszczewska, A. Jówkob and S. Matejcík. Int. J. Mass Spectrom. **314**, 42– 48 (2012).
13. F. Qi, S. Yang, L. Sheng, H. Gao, Y. Zhang and S. Yu. J. Chem. Phys. **107**, 10391 (1997).
14. MOLPRO (version 2012) is a package of ab initio programs written by H.-J. Werner, P. J. Knowles, G. Knizia, F. R. Manby, M. Schütz, P. Celani, T. Korona, R. Lindh, A. Mitrushenkov, G. Rauhut, K. R. Shamasundar, T. B. Adler, R. D. Amos, A. Bernhardsson, A. Berning, D. L. Cooper, M. J. O. Deegan, A. J. Dobbyn, F. Eckert, E. Goll, C. Hampel, A. Hesselmann, G. Hetzer, T. Hrenar, G. Jansen, C. Köppl, Y. Liu, A. W. Lloyd, R. A. Mata, A. J. May, S. J. McNicholas, W. Meyer, M. E. Mura, A. Nicklaß, D. P. O'Neill, P. Palmieri, K. Pflüger, R. Pitzer, M. Reiher, T. Shiozaki, H. Stoll, A. J. Stone, R. Tarroni, T. Thorsteinsson, M. Wang, A. Wolf. See http://www.molpro.net.
15. T. H. Dunning. J. Chem. Phys. **90**, 1007 (1989).
16. R. A. Kendall, T. H. Dunning and R. J. Harrison. J. Chem. Phys. **96**, 6796 (1992).
17. D. Figgen, K. A. Peterson, M. Dolg, and H. Stoll, J. Chem. Phys. **130**, 164108 (2009).
18. P. Schwerdtfeger, T. Fischer, M. Dolg, G. Igel-Mann, A. Nicklass, H. Stoll, A. Haaland, J. Chem. Phys. **102**, 2050 (1995).
19. K. A. Peterson, J. Chem. Phys. 119, 11099 (2003).
20. P. Schwerdtfeger, J. R. Brown, J. K. Laerdahl and Hermann Stoll, J. Chem. Phys. 113, 7110 (2000).
21. H.-J. Werner and P. J. Knowles, J. Chem. Phys. **82**, 5053 (1985).

22. P. J. Knowles and H.-J. Werner, Chem. Phys. Lett. **115**, 259 (1985).
23. H.-J. Werner and P. J. Knowles, J. Chem. Phys. **89**, 5803 (1988).
24. P. J. Knowles and H.-J. Werner, Chem. Phys. Lett. **145**, 514 (1988).
25. S.R. Langhoff and E.R. Davidson. Int. J. Quant. Chem. **8**, 61 (1974).
26. V. Brites, K. Franzreb, J. N. Harvey, S. G. Sayres, M. W. Ross, D. E. Blumling, A. W. Castleman, Jr.d and M. Hochlaf. Phys. Chem. Chem. Phys. **13**, 15233–15243 (2011).
27. J. H. D. Eland, R. Feifel, and M. Hochlaf, J. Chem. Phys. **128**, 234303 (2008).
28. H. Hammami, O. Yazidi, M. Ben El Hadj Rhouma, M. M. Al Mogren, and M. Hochlaf. J. Chem. Phys. **141**, 014302 (2014).
29. R. Llusar, M. Casarrubios, Z. Barandiarán and L. Seijo. J. Chem. Phys. **105**, 5321 (1996).
30. T. Zeng, D.G. Fedorov, M.W. Schmidt and M. Klobukowski. J. Chem. Phys. **134**, 214107 (2011).
31. A. Berning, M. Schweizer, H-J Werner, P.J. Knowles, and P. Palmieri. Mol. Phys. **98**, 1823 (2000).
32. B. Numerov. Publs. observatoire central astrophys. Russ. v. 2. 1933. p. 188.
33. J. W. Cooley, Math. Comput. **15**, 363 (1961).
34. D. D. Laun and C. H. Corliss, J. Res. Natl. Bur. Stand. (U.S.) **72**, 609 (1968).
35. J. O. Ekberg, R. Kling, and W. Mende, Phys. Scr. **61**, 146 (2000).
36. A.E. Kramida and T. Shirai. Atomic Data and Nuclear Data Tables **95**, 305–474 (2009).
37. A. E. Kramida and T. Shirai. J. Phys. Chem. Ref. Data **35**, 423–683 (2006).
38. David R. Lide, CRC Handbook of Chemistry and Physics, CRC, 2009, 89e éd., p. 10-203
39. K. Balasubramanian. J. Chem. Phys. **112**, 7425 (2000).

Figure captions:

Figure 1: Λ–Σ MRCI+Q/aug-cc-pV5Z(-PP) potential energy curves of the lowest WC^{2+} states vs. the internuclear distance. The reference energy corresponds to the energy of the ground state at equilibrium.

Figure 2: Ω potential energy curves of WC^{2+} after consideration of the spin-orbit effect. These curves are given in energy relative to the energy of WC^{2+} (X Ω = 1) at equilibrium. The dissociation limits are denotes as DL1 = $W^+(^6D_{1/2}) + C^+(^2P_{1/2})$; DL2 = $W^+(^6D_{3/2}) + C^+(^2P_{1/2})$; DL3 = $W^+(^6D_{5/2}) + C^+(^2P_{1/2})$; DL4 = $W^+(^6D_{7/2}) + C^+(^2P_{1/2})$; DL5 = $W^+(^6D_{9/2}) + C^+(^2P_{1/2})$; DL6 = $W^+(^6S_{5/2}) + C^+(^2P_{1/2})$; DL7 = $W^+(^4F_{3/2}) + C^+(^2P_{1/2})$ and DL8 = $W^{2+}(^5D_0) + C(^3P_0)$.

Figure 3: Outermost molecular orbitals (MOs) of WC obtained at the CASSCF/aug-cc-pVDZ(-PP) level.

Figure 4: Potential energy curve of WC^{2+} ground state without (upper trace) and with (lower trace) spin-orbit corrections. We locate also the v=0 level.

Table 1: Computed separation energies of W, W^+, W^{++} and their comparison with experimental data.

				CASSCF/ aug-cc-pV5Z(-PP)		MRCI/ aug-cc-pV5Z(-PP)		Exp.
Spin-orbit state	CASSCF	MRCI	MRCI+Q	$H_{el} + H_{SO}$ (u.a)	ΔE_{SO} (cm^{-1})	$H_{el} + H_{SO}$ (u.a)	ΔE_{SO} (cm^{-1})	
W								
$^5D_0$	-66.70741366	-66.795218713	-66.79961593	-66.72872247	0.00	-66.81933695	0.00	0.00
$^5D_1$				-66.72319712	1212	-66.81243774	1514	1670 [a]
$^7S_3$	-66.71892273	-66.806974112	-66.81096024	-66.71892279	2150	-66.80697411	2713	2951 [a]
$^5D_2$				-66.71571268	2855	-66.80407781	3348	3325 [a]
$^5D_3$				-66.70736567	4687	-66.79575972	5174	4830 [a]
$^5D_4$				-66.70056409	6180	-66.78807305	6861	6251 [a]
$^3P_0$	-66.64760669	-66.747603080	-66.75302505	-66.67667948	11422	-66.77546223	9629	9258.06 [a]
$^3P_1$				-66.65546506	16076	-66.75460320	14207	13307.10 [a]
$^3F_2$				-66.63751064	20018	-66.73955774	17509	-
$^3P_2$				-66.62777929	22154	-66.72920724	19781	19253.56 [a]
$^3F_3$				-66.62489203	22788	-66.72524305	20651	-
W^+								
$^6D_{1/2}$	-66.45412234	-66.516000686	-66.51775295	-66.47143243	0.00	-66.53535940	0.00	0.00 [b]
$^6D_{3/2}$				-66.46721340	925.97	-66.53051372	1063.50	1518.83 [b]
$^6D_{5/2}$				-66.46089817	2312.00	-66.52339425	2626.05	3172.47 [b]
$^6D_{7/2}$				-66.45307716	4028.52	-66.51498393	4471.90	4716.28 [b]
$^6D_{9/2}$				-66.44434593	5944.80	-66.50694782	6235.62	6147.1 [b]

$^6S_{5/2}$	-66.45403909	-66.516208613	-66.51799875	-66.41832260	11656.2	-66.48946330	10073.0	7420.26 [b]
W^{++}								
$^5D_0$	-65.90326075	-65.942890699	-65.94344171	-65.93040065	0.00	-65.97266422	0.00	0.00 [c]
$^5D_1$				-65.92366680	1477.91	-65.96497739	1692	2256.20 [c]
$^5D_2$				-65.91370514	3664.24	-65.95408787	4111	4461.19 [c]
$^5D_3$				-65.90324217	5960.60	-65.94394671	6299	6277.81 [c]
$^5D_4$				-65.89512733	7741.60	-65.93169963	7467	7686.68 [c]
$^3P_0$	-65.85659746	-65.90432859340	-65.90513718	-65.87534223	12083.92	-65.92195730	11137	9904 [c]
$^3P_1$				-65.86453127	14456.66	-65.91153811	13424	12881 [c]
$^3P_2$				-65.84806533	18070.51	-65.89746778	16512	16621 [c]

a. Ref. [34].

b. Ref. [35].

c. Ref. [36].

Table 2: First and second ionization energies (IE1 and IE2, in eV) of tungsten atom.

	W(^7S_g)		W(^5D_g)	
Method/basis set	IE1	IE2	IE1	IE2
MRCI/aug-cc-pV5Z(-PP)	7.87	23.44	7.55	23.12
MRCI+Q/aug-cc-pV5Z(-PP)	7.60	22.70	7.62	23.22
MRCI+SO/aug-cc-pV5Z(-PP)	7.60	22.70	7.93	23.04
Exp.			7.86403 [a)]	23.96 [a)]

a. Ref. [38].

Table 3: Dominant electron configuration of the lowest electronic states of WC^{2+} investigated presently quoted at the equilibrium distance of $WC^{2+}(X^3\Delta)$. T (in eV) is the vertical excitation energy with respect to $WC^{2+}(X^3\Delta)$ minimum energy.

State	Dominant electron configuration	T
$X^3\Delta$	$\ldots 4\sigma^2\, 2\pi^4\, 5\sigma^1\, 1\delta^1\, 6\sigma^0$	0.00
$1^3\prod$	$\ldots 4\sigma^2\, 2\pi^3\, 5\sigma^2\, 1\delta^1\, 6\sigma^0$	0.80
$1^3\Phi$	$\ldots 4\sigma^2\, 2\pi^3\, 5\sigma^2\, 1\delta^1\, 6\sigma^0$	0.89
$1^5\prod$	$\ldots 4\sigma^2\, 2\pi^3\, 5\sigma^1\, 1\delta^2\, 6\sigma^0$	0.91
$1^5\sum^+$	$\ldots 4\sigma^2\, 2\pi^2\, 5\sigma^2\, 1\delta^2\, 6\sigma^0$	1.30
$1^3\sum^+$	$\ldots 4\sigma^2\, 2\pi^4\, 5\sigma^1\, 1\delta^0\, 6\sigma^1$	1.65
$1^7\sum^+$	$\ldots 4\sigma^2\, 2\pi^2\, 5\sigma^1\, 1\delta^2\, 6\sigma^1$	1.85
$1^3\sum^-$	$\ldots 4\sigma^2\, 2\pi^4\, 5\sigma^0\, 1\delta^2\, 6\sigma^0$	2.13
$1^5\Delta$	$\ldots 4\sigma^2\, 2\pi^2\, 5\sigma^2\, 1\delta^1\, 6\sigma^1$	2.19
$1^7\prod$	$\ldots 4\sigma^2\, 2\pi^2\, 5\sigma^1\, 1\delta^2\, 6\sigma^0\, 3\pi^1$	2.57
$1^7\Delta$	$\ldots 4\sigma^2\, 2\pi^2\, 5\sigma^1\, 1\delta^1\, 6\sigma^0\, 3\pi^2$	3.48

Table 4: Adiabatic excitation energy (T_0, in eV), equilibrium distances (R_e, in Å), rotational (B_e, α_e) and vibrational (G_0, ω_e, $\omega_e x_e$) constants (in cm^{-1}) of the lowest electronic states of $^{184}W^{12}C^{2+}$ with (Ω states) and without (Λ–Σ states) considering the spin-orbit effect.

State	T_0	R_e	ω_e	$\omega_e x_e$	G_0	B_e	α_e
Λ - Σ states							
$X^3\Delta$	0.00 [a)]	1.736	1008.2	8.1	511.3	0.4961	0.0039
$1^3\prod$	0.80	1.820	835.1	-1.9	417.5	0.4510	0.0027
$1^3\Phi$	0.89	1.817	842.6	-2.4	421.1	0.4528	0.0028
$1^5\prod$	0.91	1.863	817.7	-5.6	407.2	0.4309	0.0031
$1^5\sum^+$	1.30	1.967	663.7	-4.2	331.0	0.3865	0.0033
$1^3\sum^+$	1.65	1.757	1136.4	1.1	566.5	0.4822	-0.0023
$1^7\sum^+$	1.85	2.032	636.6	-4.9	317.0	0.3622	0.0032
$1^3\sum^-$	2.13	1.856	1261.3	-	314.8	0.4341	-0.0349
$1^5\Delta$	2.19	2.040	583.1	-4.2	290.5	0.3594	0.0032
$1^7\prod$	2.57	2.040	636.6	-4.9	317.0	0.3622	0.0032
$1^7\Delta$	3.48	2.553	302.4	-3.7	150.4	0.2294	0.0031
Ω states							
X Ω=1	0.00 [a)]	1.744	1003.6	4.3	503.6	0.4917	0.0000
1 Ω=2	0.27	1.747	992.8	3.4	497.5	0.4900	-0.0002
1 Ω=3	0.52	1.755	947.2	-7.6	468.8	0.4856	0.0009
2 Ω=1	0.83	1.791	1292.2	-77.8	603.6	0.4663	-0.0047
1 Ω=0	0.97	1.882	1016.7	-64.6	488.9	0.4225	-0.0145
2 Ω=2	1.11	1.865	819.1	-1.6	410.5	0.43010	0.0035
2 Ω=3	1.15	1.909	962.2	-54.8	454.9	0.41044	-0.0075
2 Ω=0	1.17	1.824	1149.1	-	518.8	0.44961	0.0071
3 Ω=2	1.15	1.842	980.6	31.4	507.7	0.4409	-0.0041
3 Ω=1	1.54	1.845	902.3	-37.5	435.7	0.4394	0.0068
3 Ω=0	2.11	1.951	1085.2	-17.5	533.7	0.3933	-0.0044

a. Used as reference.

Figure 1

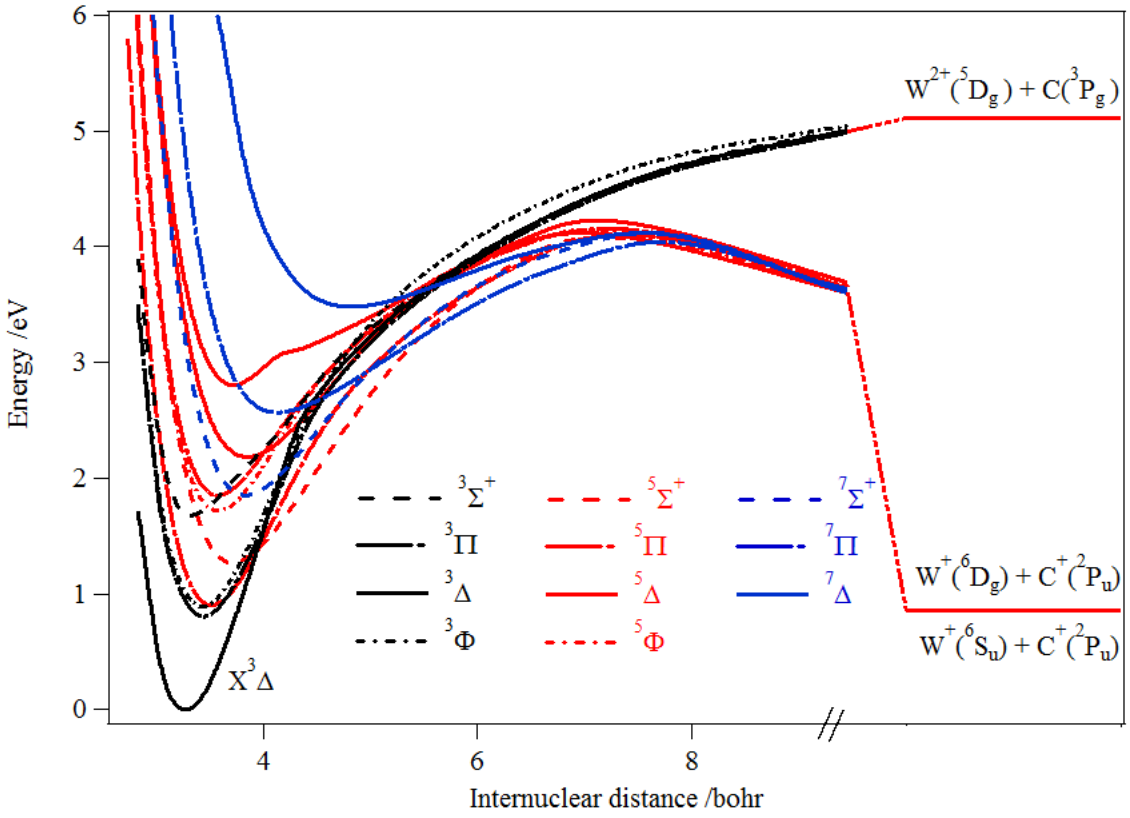

Figure 2

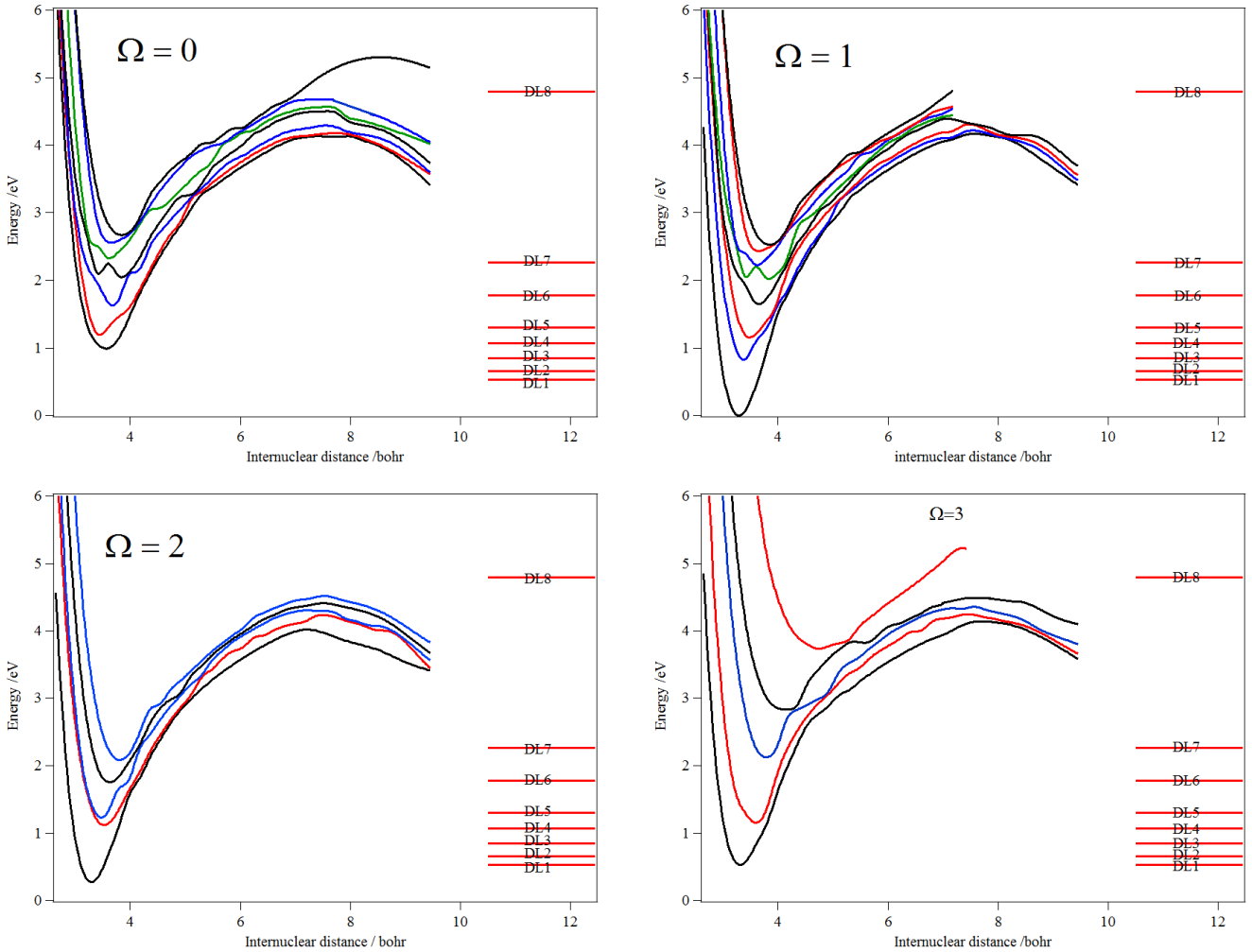

Figure 3

5σ MO	1δ MO	6σ MO
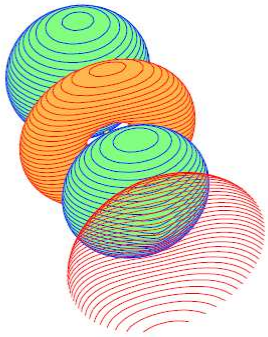	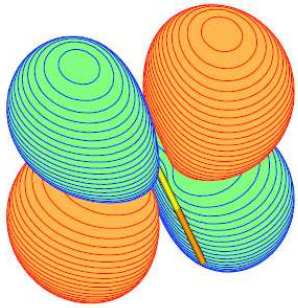	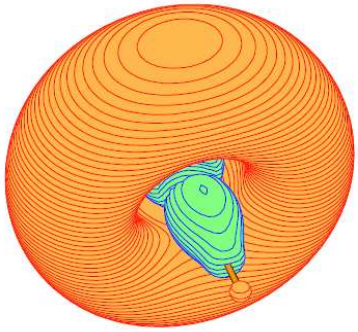

Figure 4